Proceedings of the 28th IEEE
EMBS Annual International Conference
New York City, USA, Aug 30-Sept 3, 2006

New Applications of Planar Image Fusion in Clinical Nuclear Medicine and Radiology

Lionel S. Zuckier, and Holly M. Koncicki

Abstract—**Fusion of multiple modalities has become an integral part of modern imaging methodology, especially in nuclear medicine where PET and SPECT scanning are frequently paired with computed tomography (CT). We have extended image fusion from the tomographic realm to planar imaging in 2 specific applications. In the first, we combine planar scintigraphic images with photographic images of the body part of interest, using a predetermined transformation of images between the frames of reference. This technique is especially helpful in "hot spot" imaging applications where minimal background activity makes it difficult to locate abnormalities in an anatomic context. The technique has been demonstrated to be accurate, and results in increased reader confidence. We have also begun fusing orthopedic radiographs with photographic images of the extremities, using fiducial markers within each image set to perform an affine transformation unique for the particular image set. Preliminary results indicate that this method is accurate, and clinical evaluation is underway.**

I. Introduction

In the last decade, there has been a fundamental shift in medical imaging. Rather than viewing various imaging techniques as disparate and independent sources of information, researchers have begun to combine these data in new and innovative ways. At least in part, these efforts have been facilitated by shared image standards, specifically DICOM [1-3], which has provided a lingua franca for medical imaging.

The fusion of functional images derived from Positron Emission Tomography (PET) and Single Photon Emission Computed Tomography (SPECT) with anatomic images, such as Computed Tomography (CT), has been shown to increase the accuracy and certainty of localizing lesions, and has become dominant in the commercial marketplace [4-7]. The combination of functional and anatomic imaging modalities is especially synergistic in that each modality compliments the other to remedy a specific weak point. Spatial resolution of PET and SPECT imaging is relatively poor, while that of CT imaging is excellent. CT imaging is relatively insensitive to dynamic processes and physiologic states; however, PET and SPECT imaging are based on the radioactive tracer principle and excel at elucidating physiologic processes within the body. In this way the fusion of PET or SPECT with CT serves to create a very robust hybrid.

Manuscript received May 24, 2006.

L. S. Zuckier is with the Department of Radiology, New Jersey Medical School – UMDNJ, Newark, NJ 07101 USA (phone: 973-972-6023; fax: 973-972-6954; e-mail: zuckier@umdnj.edu).

H. M. Koncicki is completing second year studies as a medical student with the New Jersey Medical School – UMDNJ, Newark, NJ 07101 USA (e-mail: koncichm@umdnj.edu). This work was supported by a Cancer Education Research Traineeship from the National Cancer Institute.

Initial attempts to retrospectively combine imaging data between modalities were stymied by difficulties in registering images obtained at different times with patients in differing postures and with differing abdominal contents [8]. Eventually, camera vendors developed integrated systems where multiple modalities were combined into one unit which facilitates nearly simultaneous imaging. Additional synergy was obtained by translating the CT image density map to provide an estimated attenuation correction for the PET or SPECT photons, thereby bypassing the need for acquiring the time-consuming and noisy transmission attenuation scan that had been the standard practice.

An area in nuclear medicine imaging where fusion with anatomic modalities has not penetrated is planar scintigraphy. Fusion with an anatomic modality would be especially helpful in "hot spot" imaging applications, where abnormalities are apparent as areas of uptake on a background of very little activity (fig. 1). In these cases, the low background activity makes it difficult to discern normal anatomic structures and thereby site the hot spots. Examples of hot-spot imaging include the imaging of thyroid cancer with radioactive iodide, imaging of radiolabelled white blood cells, and lymphoscintigraphy.

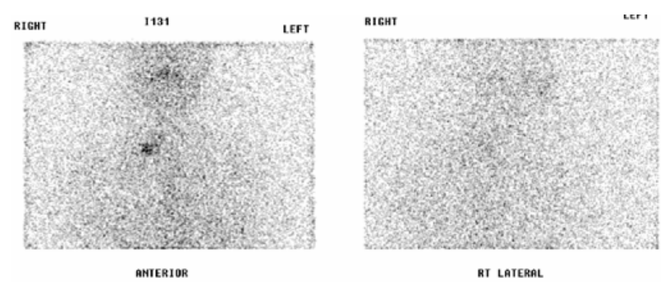

Fig. 1. Example of "hot spot" imaging. Anterior (left panel) and right lateral (right panel) views centered over the neck demonstrate a focus of concentration of ^{131}I-NaI due to functioning thyroid tissue. Lack of background activity makes precise anatomic localization difficult.

Because of this need, we have applied fusion techniques to planar radionuclide scintigraphy, combining these images with photographic images of the areas of interest. We have also identified orthopedic oncology as an additional application in which a visual fusion system would be beneficial. Presently, in the operating room (O.R.), fluoroscopy is used to localize bone tumors and direct the surgical approach. By allowing the surgeon to localize the tumor based on visual surface features, previously performed fusion imaging may eliminate the need for fluoroscopy, thereby reducing time in the O.R. and decreasing radiation exposure, while maintaining accuracy of localization. In fusion of visual and scintigraphic images, we are combining a functional and anatomic modality as in the tomographic examples previously discussed. In the fusion of radiographs and visual images, we are in fact combining 2 forms of anatomic information.

II. Planar Scintigraphic and Visual Imaging Fusion

A. Method

We have previously described our method of combining planar scintigraphic and visual images [9-10]. This project was approved by the New Jersey Medical School Institution Review Board (IRB). We installed a 2.11 megapixel camera 255 cm above the floor, directly over the gamma camera (fig. 2). The camera is remotely controlled by public domain software, which allows for control of zoom, resolution, flash, exposure, and image retrieval over a serial cable [11]. Instructions were simplified by means of scripted and menued batch commands.

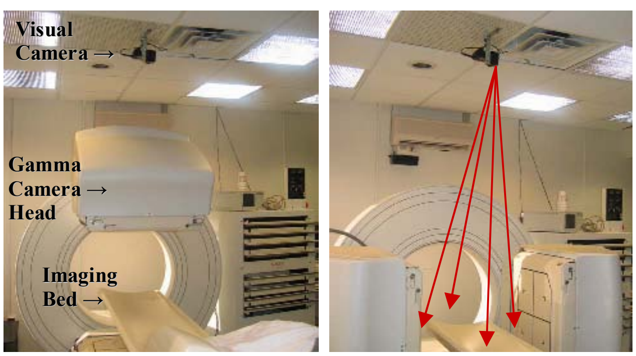

Fig. 2. Physical design of scintigraphic/visual camera system. The visual camera (Nikon Coolpix 850) is attached to the ceiling above the gamma camera (Philips, Forte system) and is remotely controlled by software batch commands. In the left panel, the gamma camera is positioned to obtain the scintigraphic image. Heads are then rotated by 90° and the visual photograph is obtained (right panel) with the patient at a fixed distance (128 cm) from the visual camera, and prior to any patient movement.

All patients gave informed consent to participate in this study. Photographic and scintigraphic images were retrieved to the hard drive for registration and fusion. Our method was initially developed in the MatLab environment (The MathWorks, Natick, MA), and was subsequently ported to ImageJ, using TurboReg and Image Layering plugins [12]. Registration of the scintigraphic image with the photographic image was performed using an affine transformation, parameters of which were defined by prior imaging of a phantom consisting of 3 fiducial cobalt-57 markers (fig. 3).

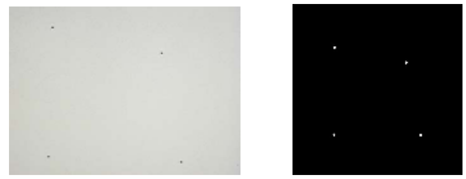

Fig. 3. Visual (left panel) and scintigraphic (right panel) images of a registration phantom. The 3 outer markers are used to define the affine transformation, mapping from the visual to the scintigraphic coordinates (the additional 4th point was used as a measure of accuracy and is not further described in this review). Once defined, the registration parameters were used to transform subsequent clinical images.

B. Clinical Applications

Selected illustrative examples of this method are illustrated below (fig. 4-6).

Fig. 4. In this patient with thyroid carcinoma, initial iodide I-123 image demonstrates 2 “hot spots” that are difficult to localize due to paucity of background counts (left panel). Registration and fusion of the patient’s photographic image allows for accurate localization (arrowheads). Images are best seen on color display.

Fig. 5. In this patient with thyroid carcinoma, exact location of the several foci of ^{131}I-NaI uptake is difficult (left panel). Planar fusion reveals foci in the neck, chest, and right arm (arrow). Faint lung uptake is also noted.

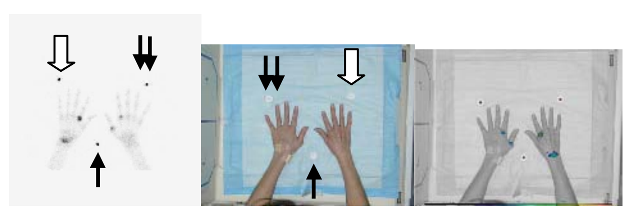

Fig. 6. In a variation of the method, extremities can be imaged using a gamma-camera head under the area of interest (gamma-camera image grayscale is inverted in this example). Three fiducial markers (arrows) have been placed on the image and used to register the activity from below the patient to the visual image obtained from above. Note change in orientation between the 2 images, taken from above and below the hands. Arthritic changes are mapped to the involved joints.

C. Validation

In a subset of patients, a single Co-57 marker was placed on the area of clinical interest as a surrogate focus to estimate error of registration (fig. 7). In a total of 10 patients studied, mean root square error was 1.3 pixels corresponding to 3.1 mm and never exceeded 2.2 pixels (5.2 mm).

Fig. 7. A subset of patient images was obtained with Co-57 radioactive markers placed on the areas of interest (arrow), thereby allowing accuracy of registration to be estimated. In the example displayed, location of the marker varied between the translated visual and scintigraphic image by a single pixel in each of the X and Y coordinates, corresponding to an error of approximately 3.3 mm.

As well, a clinical evaluation was performed based on subjective rating by radiologist trainees. Nine radiology residents were shown 2 panels of 15 cases (thyroid, lymphoscintigraphy and orthopedic), the first consisting of scintigraphic images alone and the second of scintigraphic and fused images, presented in a shuffled order. Residents rated confidence of their interpretation for each image on a 5 point scale. Mean confidence levels were compared for panels with and without fusion images (fig. 8) and increased when fusion images were added to standard scintigraphic images.

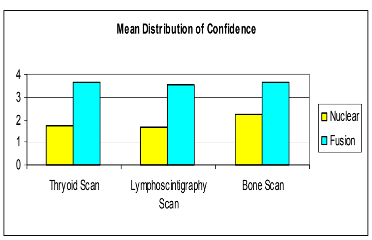

Fig. 8. Mean distribution of confidence for accurately localizing areas of uptake using scintigraphic images alone or scintigraphic images plus fusion in 3 subsets of clinical applications (0 least confident and 4 most confident). Confidence increases when fusion images were added to standard scintigraphic images.

III. Planar X-ray and Visual Imaging Fusion

In this newly developed technique, we describe our method of fusing clinical radiographs with visual images.

A. Method

Permission to perform this study on patients was obtained from the New Jersey Medical School IRB. A subset of patients obtaining x-rays of the extremities was asked to participate in the study and signed informed consent.

A 2.11 megapixel camera (Nikon Coolpix 850) was affixed to the side of the X-ray tube assembly using a magnetic mount. The field of view of the camera was aligned with the field of view of the x-ray unit using a variable zoom and f stop of 3.0. The radiograph was taken using standard parameters. Immediately thereafter, prior to moving the patient, the x-ray tube assembly was shifted laterally by 24 cm in order to center the visual camera over the x-ray field-of-view.

To allow registration of the x-ray images with the visual images, 3 commercially-available adhesive disposable fiducial markers (Beekley Spots, Bristol CT) were placed on the periphery of the extremity imaged, so as not to obstruct the diagnostic radiograph (fig. 9).

Fig. 9. Xray and photograph (2 leftmost panels) of the patient's lower leg are shown, indicating position of disposable fiducial markers (arrows). There were used to generate an affine registration, registering the x-ray to the visual image. There were then fused and displayed according to various protocols (2 right panels). The last panel is best seen in a color display.

Subsequently, because of the difficulty in finding 3 non-obtrusive locations on the patient's extremities, markers external to the body were used. In these instances, wooden blocks, approximately 1 cm^3 in size, were placed into 3 stacks that approximated the height of the extremity imaged, upon each was placed a Beekley Spot marker. When possible, an extra fourth marker was placed on the extremity itself to serve as a surrogate lesion for measurement of accuracy of registration (fig. 10).

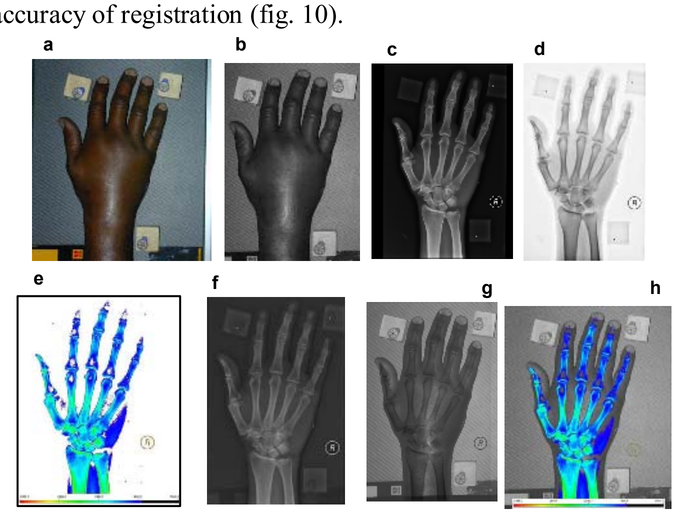

Fig. 10. The more recent technique is displayed, where fiducial markers are placed on wooden blocks external to the patient. Wherever possible, an additional single marker was placed unobtrusively on the patient's skin, to serve as a surrogate lesion for measurement of accuracy of registration. Various images indicated in the diagram include: (a) digital color visual image, (b) grayscale visual image, (c) positive x-ray, (d) negative x-ray, (e) color coded positive x-ray, (f) fused image (b+c), (g) fused image (b+d), (h) fused image (b+e)

ImageJ software was used for registration and fusion. Images were converted to grayscale and an affine registration was performed, mapping the radiograph to the visual coordinate system, using the 3 fiducial markers. The aligned images were then fused using several color-coded protocols within the Image Layering Toolbox plugin. Where present, pixel location of the fourth marker was determined on the photographic image and transformed radiograph, and any discrepancies noted. Pixel distance between the locations was calculated and converted into millimeters. In this manner, mean and standard deviation of the error were determined in 11 patients.

B. Results:

A total of 37 images in 18 patients have been performed. Examples using fiducial markers on the patient (fig. 9) and external to the patient (fig. 10) are presented. Fusion of grayscale visual images to negative (inverted) radiographs appears to be the clearest mode of display (fig. 10). Mean and standard deviation of the error of the surrogate markers was determined to be 1.5 ± 0.7 mm. In no patient was the error greater than 2.7 mm.

IV. Conclusion

We have demonstrated the feasibility and accuracy of planar fusion in 2 applications, planar scintigraphy, and radiography of the extremities, using readily available software. Further evaluation of clinical impact is underway.

Acknowledgment

We wish to acknowledge the authors of the following software: PhotoPC Software for PC control of Nikon camera (http://www.lightner.net/lightner/bruce/photopc/), ImageJ software (http://rsb.info.nih.gov/ij/index.html), and ImageJ plugins TurboReg (Philippe Thévenaz, Biomedical Imaging Group, Swiss Federal Institute of Tech., Lausanne) and Image Layering Toolbox (Karl Schmidt, HypX Laboratory, Brigham and Women's Hospital, Boston).

References

[1] Flanders, A. E. and Carrino, J. A., "Understanding DICOM and IHE," *Semin Roentgenol*, vol. 38, no. 3, pp. 270-281, 2003.

[2] Bidgood, W. D., Jr., Horii, S. C., Prior, F. W., and Van Syckle, D. E., "Understanding and using DICOM, the data interchange standard for biomedical imaging," *J Am Med Inform Assoc*, vol. 4, no. 3, pp. 199-212, 1997.

[3] Graham, R. N., Perriss, R. W., and Scarsbrook, A. F., "DICOM demystified: a review of digital file formats and their use in radiological practice," *Clin Radiol*, vol. 60, no. 11, pp. 1133-1140, 2005.

[4] Israel, O., Keidar, Z., Iosilevsky, G., Bettman, L., Sachs, J., and Frenkel, A., "The fusion of anatomic and physiologic imaging in the management of patients with cancer," *Semin Nucl Med*, vol. 31, no. 3, pp. 191-205, 2001.

[5] Keidar, Z., Israel, O., and Krausz, Y., "SPECT/CT in tumor imaging: technical aspects and clinical applications," *Semin Nucl Med*, vol. 33, no. 3, pp. 205-218, 2003.

[6] Schillaci, O., "Hybrid SPECT/CT: a new era for SPECT imaging?," *Eur J Nucl Med Mol Imaging*, vol. 32, no. 5, pp. 521-524, 2005.

[7] von Schulthess, G. K., Steinert, H. C., and Hany, T. F., "Integrated PET/CT: current applications and future directions," *Radiology*, vol. 238, no. 2, pp. 405-422, 2006.

[8] Levin, D. N., Pelizzari, C. A., Chen, G. T., Chen, C. T., and Cooper, M. D., "Retrospective geometric correlation of MR, CT, and PET images," *Radiology*, vol. 169, no. 3, pp. 817-823, Dec.1988.

[9] Zuckier, L. S., Puthiamadathil, J. M., Dhawan, A. P., Ghesani, N. V., and Vazirani, T. Scintigraphic/visual fusion imaging for improved localization of thyroid abnormalities: method, proof of principle and preliminary evaluation. Journal of Nuclear Medicine 46, 318p. 2005.

[10] Puthiamadathil, J. M., Zuckier, L. S., and Dhawan, A. P. Planar visual fusion scintigraphy. Proceedings, 26th Annual International Conference of the IEEE Engineering in Medicine and Biology Society, San Francisco. 2004.

[11] Wunsam, S. and Bowman, J. C. Economical digital photomicroscopy. Journal of Paleolimnology 25[3], 399-403. 2001.

[12] Abramoff, M. D., Magelhaes, P. J., and Ram, S. J., "Image processing with ImageJ," *Biophotonics International*, vol. 11, no. 7, pp. 36-42, 2004.